Investigation of the High Power Integrated Uni-Traveling Carrier and Waveguide Integrated Photodiode

T. S. Liao, P. Mages, P. K. L. Yu
Dept. of Electrical and Computer Engineering, University of California, San Diego, CA 92093
E. W. Jacobs, J.B. Sobti
SPAWAR Systems Center, San Diego, CA 92152-5001

Abstract

A uni-traveling carrier waveguide integrated photodiode (UTC-WIP) combining the advantages of a coupled waveguide integrated photodiode (WIP) [1-2] and a uni-traveling carrier photodiode (UTC-PD) [3-6] is investigated. Preliminary measurement results show that the DC responsivity is 0.4 A/W without anti-reflection coating, and the peak pulse response can reach 94 mA (4.7 V across a 50 Ω load) when the bias voltage is –9 V. The resulting device is capable of operating at 20 GHz. The IP_3 at 1 GHz and 18 GHz are 24 dBm and 8 dBm, respectively.

Introduction

High RF link gain, low noise figure and high spurious free dynamic range (SFDR) are desirable for analog fiber optic links. All of these properties can be easily obtained if the components can operate at a high optical power level [7-8]. A large bandwidth is desirable for large channel capacity. This implies that the link components, including the photodiode, must have high saturation power and wide bandwidth. In addition, if the pulse response of the photodiode shows a high peak response, short rise-time, and a long fall-time, this device can be used as a high isolation switch in applications, such as the track-and-hold circuit for analog to digital converters [9].

The saturation power of a photodiode is mainly attributed to the space charge screening effect due to the dense photogenerated carriers [10-11]. In the conventional waveguide photodiode, the distribution of photogenerated carriers usually follows an exponential decay profile along the absorption layer which leads to a high density of photogenerated carriers at the front end. To mitigate this problem so as to increase the saturation power as well as the bandwidth, two types of photodiodes have been developed, namely the coupled waveguide integrated photodiode (WIP)[1-2] and the uni-traveling carrier photodiode (UTC-PD)[3-6].

In the WIP design, the use of a matching layer allows for a gradual enhancement of the optical confinement factor $\Gamma(z)$ along the waveguide. Thus absorption can be designed to be evenly distributed to minimize the dense absorption at the front end.

Since the velocity of electrons is higher than that of holes [12], the UTC concept [3] can be used wherein the photo-generated electrons are swept out quickly while the photogenerated holes merge with the other majority carriers instantly. This reduces the excess charge density, thereby lessening the charge screening effect. Based on this principle, in the UTC-PD, the absorber is in a p-doped layer (P-layer) instead of in an intrinsic layer (I-layer) as is in the case of the conventional P-I-N photodiode. The electrons need to move through the P-layer and the I-layer to the n-doped layer.

Since the WIP and UTC-PD use different approaches to improve the saturation power, it is worthwhile to investigate the combined effect in a single device. Our study shows that such a uni-traveling carrier waveguide integrated photodiode (UTC-WIP) can be easily fabricated. Preliminary measurements of the photodiode show that DC responsivity is 0.4 A/W. In addition, the peak pulsed voltage response across a 50 Ω load can reach 4.7 V (94 mA) when the bias voltage is –9 V. The bandwidth of this device is in excess of 20GHz. The IP_3 at 1 GHz and 18 GHz are 24 dBm and 8 dBm, respectively.

UTC-WIP Design

0-7803-7695-1/03/$17.00 © 2003 IEEE

In this work, a UTC-WIP with an index matching layer and P-layer absorber, as shown in Fig.1 is investigated to achieve distributed absorption and fast carrier sweep out. In this device, due to the index matching layer, the confinement factor $\Gamma(z)$ varies periodically along the absorber as in multi-mode beating. The beam propagation method (BPM) simulator (distributed by R-soft Research, Inc) is used to design the p-layer and the index matching layer thickness [2]. The results show the p-layer needs to be thick enough so that effective distributed absorption can be achieved within a relatively short propagation distance.

Considering the operation of the UTC-PD, the photogenerated electrons need to diffuse through the P-layer and drift through I-layer to N-layer. The diffusion time can be expressed as:

$$t_{diff} = \frac{W_P^2}{2D_e} \qquad (1)$$

where W_p is the P-layer thickness and D_e is the electron diffusivity in InGaAs. It is noted that the diffusion time is proportional to the square of the P-layer thickness. The speed can be improved by adding a drift component to the electron transport [17].

The speed of this photodiode is also determined by the electron drift time in the I-layer and the RC time constant.

The optimized P-layer and I-layer thicknesses with respect to both the bandwidth and power absorption are 0.2 μm and 0.45 μm respectively. With these P-layer and I-layer thicknesses in the UTC-WIP design, over 80% of the illuminated power will be absorbed within 70 μm, while estimated bandwidth of this device is 34 GHz.

Performance

The RF responsivity of the UTC-WIP was measured with a HP8703 lightwave vector network analyzer with a sweeping bandwidth from 300 MHz to 20GHz. When the UTC-WIP with 70 μm long absorber was biased at –5 V, the 3 dB bandwidth is observed to be larger than 20 GHz as shown in Fig 2. The frequency response at 20GHz is about 1.5 dB lower than the low frequency value.

In high performance analog fiber optic links, the nonlinear distortions, which get worse when the photodiode is saturated, limit the SFDR [14]. In order to characterize the nonlinear distortion of the UTC-WIP, two-tone measurements using two lasers and two Mach Zehnder modulators [15] were carried out to extract the output referenced 3rd order intercept point (IP_3) of the UTC-WIP.

The two-tone measurements were performed with f_1 and f_2 set at 1 and 1.01 GHz, and also at 18 and 18.01 GHz, biased at –5 V. The output referenced IP_3 was extrapolated from the fundamental signals and the IMD_3's. The extracted IP_3 are 24 dBm at 1 GHz and 8 dBm at 18 GHz with 1.8 mA photocurrent as shown in Fig 3. The SFDR of this photodiode (shot-noise limited) was 128 $dB/Hz^{2/3}$ at 1 GHz and 117 $dB/Hz^{2/3}$ at 18 GHz, respectively.

To characterize the pulse response of the UTC-WIP, a pulse response measurement has been done. In this measurement, a 5 ps light pulse with 960 MHz pulse repetition rate from a 1.55 μm mode-locked laser was launched into the UTC-WIP biased at different voltage levels. The results show that when a –9V bias voltage and 25 pJ/pulse are applied to the UTC-WIP, a peak voltage of 4.7 V across a 50 Ω load is measured as shown in Fig 4.

Equivalent Circuit Model and Power Transmission

An equivalent circuit model of the photodiode is shown in Fig 5, where R_j is the junction resistance, C_j is the junction capacitance, R_s is the contact resistance and C_p is the parasitic capacitance. It has been shown experimentally that in conventional WIP photodiode optical power illumination caused a variation of R_j and C_j [16].

In reference to the equivalent circuit model, the power transmitted to the load at frequency ω can be expressed as:

$$P_L = \frac{1}{2} \cdot \frac{I_g^2 \cdot R_j^2 \cdot R_L}{K_1^2 + \omega^2 \cdot K_2^2} \qquad (2)$$

where P_L is the load power, I_g the photocurre nt and

$$K_1 = (R_j + R_s + R_L) - \omega^2 C_P R_L R_j C_j R_s$$
$$K_2 = C_P R_L (R_j + R_S) + R_j C_j (R_L + R_S)$$

From the Eq. (2), the power transmitted to the load is seen to be influenced by R_j. For example, assuming R_s is 25 Ω and R_L is 50Ω, if R_j is reduced from 20 kΩ to 200Ω, the power delivered to the load at very low frequency (ω=0) is reduced by 3 dB.

By curve-fitting the S_{11} measurement data, the parameters in this model can be extracted at different electrical and optical biases. Fig 5 shows the S_{11} measurement results when this photodiode is biased at –3V and the photocurrent is 3mA. The curve fitting to these data is also shown. For comparison with the WIP [2], the corresponding S_{11} at the same bias voltage and photocurrent (with the fitting curve) are also shown in Fig 5. In these two structures, the absorption profiles are similar according to the BPM simulation results. From the S_{11} measurement results, the return loss of UTC-WIP at very low frequency is 0 dB, but that of WIP is 0.5dB. This can be explained by the higher R_j of the former. The curve fitting results show that R_j of UTC-WIP is 20 kΩ, and that of WIP is only about 1.1 kΩ. However, the original R_j of WIP without any photocurrent (0 mA) is larger than 20 kΩ.

UTC-WIP and WIP share the same absorption profile, the peak current densities are similar and are estimated to be about 4.2 kA/cm^2. However, due to a faster carrier velocity in UTC-WIP, the peak photogenerated carrier density is much smaller. The estimated peak photo-generated carrier density of UTC-WIP is 2.6 x 10^{15}cm^{-3}, and that of WIP is 8.8 x 10^{15}cm^{-3}. These preliminary results show that because UTC-WIP has a faster carrier velocity, the extra carrier density becomes smaller so that R_j remains constant over the optical intensity tested. Therefore, the UTC-WIP can be operated at high power level without degrading the efficiency of the power transmission.

Conclusion

In summary, the UTC-WIP, combining the benefits of both WIP and UTC designs, shows improved linearity and high peak pulse response performance as well as high speed. This device can be used in not only an analog fiber optical links, but also as a high-speed high-power switch.

Acknowledgements

The authors would like to thank Mrs. Jessica G. H. Fischer at the University of California, San Diego for her help in measurement. This work is sponsored by the DARPA PACT and NSF ANIR program.

References

[1] L. Giraudet, S. Demiguel, F, Banfi, IEEE LEOS'99, pp. 866-867, 1999.
[2] H. Jiang and Paul K. L. Yu, IEEE MTT, Vol 48, pp. 2604-2610, 2000.
[3] T. Ishibashi, H. Fushimi, H. Ito, and T. Furuta, MWP'99 Digest, pp. 75-78, 1999.
[4] Y. Muramoto, K. Kato, M. Mitsuhara, O. Nakajima, Y. Matsuoka, N. Shimizu and T. Ishibashi., Elec. Lett., Vol 34 , pp. 122-123, 1998.
[5] H. Ito, T. Furuta, S. Kodama and T. Ishibashi, Elec. Lett., Vol 36, pp. 1809-1810, 2000.
[6] M. Yuda, K. Kato, R. Iga and M. Mitsuhara, Elec. Lett., Vol 35, pp. 1377-1379, 1999.
[7] G.E. Betts, L. M. Johnson and C. H. Cox III, Proc. SPIE, Vol. 1562, pp. 281-302, 1991.
[8] K. J. Williams, L. T. Nichols, and R. D. Esman, J. Lightwave Technol., Vol. 16, pp. 192-199, 1998.
[9] T. S. Liao, E. W. Jacobs, P. K. L. Yu, Digest of LEOS'02 Annual Meeting, pp. 536-537, 2002.
[10] A.R. Williams, A.L. Kellner, and P. K. L. Yu, IEE Electron. Lett., 29, pp. 1298-1299, 1993.

[11] J. Harari, G. Jin, J. P. Vilcot and D. Decoster, IEEE Trans. MTT, Vol 45, pp. 1332-1336, 1997.
[12] P. Hill, J. Schlafer, W. Powazink, M. Urban, E. Eichen, and R. Olshansky, Appl. Phys Lett., Vol. 50, pp.1260-1262, 1981.
[13] A. R. Williams, A. L. Kellner, X. S. Jiang and P. K. L. Yu, Elec. Lett., Vol. 28, pp. 2258-2259, 1992.
[14] T. A. Vang, et al., Digest of LEOS'99 Annual Meeting, pp. 804-805, 1999.
[15] H. Jiang, D. S. Shin, G. L. Li, J. T. Zhu, T. A. Vang, and P. K. L. Yu, IEEE Microwave Photonics Conference, MWP'99, Paper T-5.3, 1999.
[16] Jiang, H.; Shin, D.S.; Li, G.L.; Vang, T.A.; Scott, D.C.; Yu, P.K.L, IEEE Photonics Tech. Lett., Vol.12, pp. 540-542, 2000.
[17] S. M. Sze, " Modern Semiconductor Device Physics",Wiley, pp. 15, 1998.

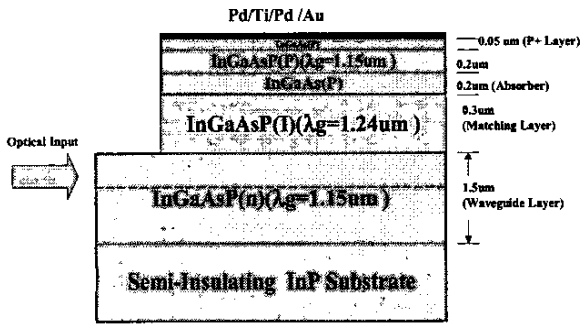

Fig 1. The layer structure of UTC-WIP

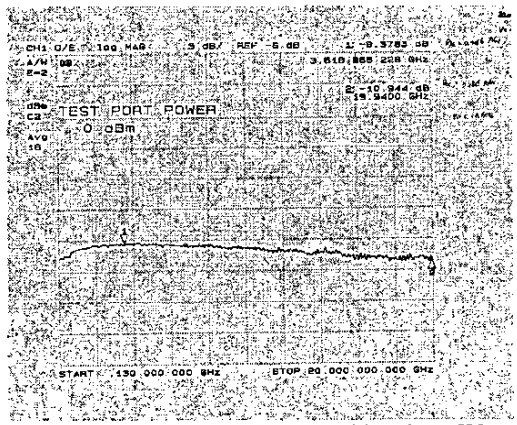

Fig 2. Bandwidth of UTC-WIP biased at –5V

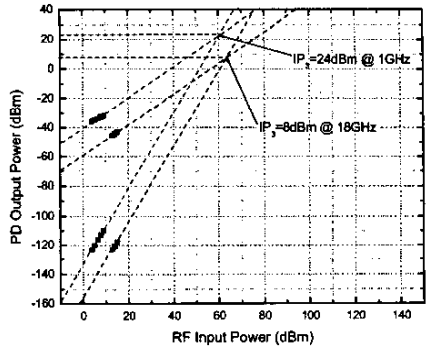

Fig 3. IP_3 of UTC-WIP at 1GHz and 18GHz

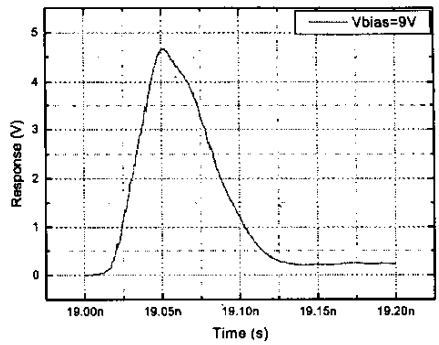

Fig 4. Pulse Response of UTC-WIP.

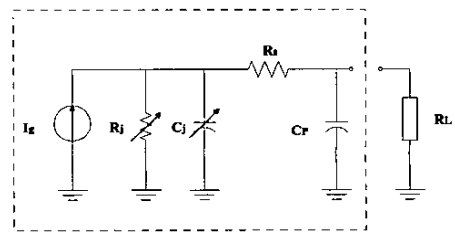

Fig 5. The equivalent circuit model of photodiode

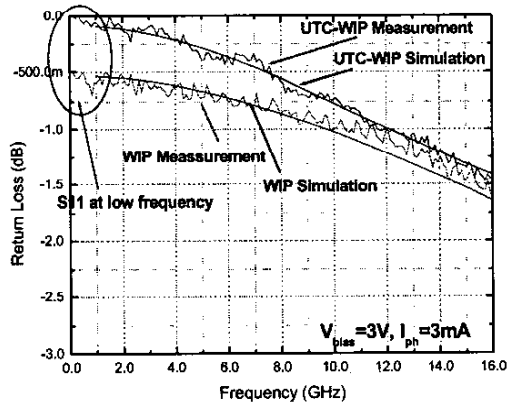

Fig 6. S_{11} measurements of UTC-WIP and WIP (Bias voltage=3V and Photocurrent=3mA)